

# Journal of Biomedical Optics

[SPIEDigitalLibrary.org/jbo](http://SPIEDigitalLibrary.org/jbo)

## **Specifying peripheral aberrations in visual science**

W. Neil Charman  
Ankit Mathur  
Dion H. Scott  
Andreas Hartwig  
David A. Atchison

# Specifying peripheral aberrations in visual science

W. Neil Charman,<sup>a</sup> Ankit Mathur,<sup>b</sup> Dion H. Scott,<sup>b</sup> Andreas Hartwig,<sup>a</sup> and David A. Atchison<sup>b</sup>

<sup>a</sup>University of Manchester, Faculty of Life Sciences, Manchester M13 9PL, United Kingdom

<sup>b</sup>Queensland University of Technology, Institute of Health and Biomedical Innovation, 60 Musk Avenue, Kelvin Grove, Q 4059 Australia

**Abstract.** Purpose: Investigations of foveal aberrations assume circular pupils. However, the pupil becomes increasingly elliptical with increase in visual field eccentricity. We address this and other issues concerning peripheral aberration specification. Methods: One approach uses an elliptical pupil similar to the actual pupil shape, stretched along its minor axis to become a circle so that Zernike circular aberration polynomials may be used. Another approach uses a circular pupil whose diameter matches either the larger or smaller dimension of the elliptical pupil. Pictorial presentation of aberrations, influence of wavelength on aberrations, sign differences between aberrations for fellow eyes, and referencing position to either the visual field or the retina are considered. Results: Examples show differences between the two approaches. Each has its advantages and disadvantages, but there are ways to compensate for most disadvantages. Two representations of data are pupil aberration maps at each position in the visual field and maps showing the variation in individual aberration coefficients across the field. Conclusions: Based on simplicity of use, adequacy of approximation, possible departures of off-axis pupils from ellipticity, and ease of understanding by clinicians, the circular pupil approach is preferable to the stretched elliptical approach for studies involving field angles up to 30 deg. © 2012 Society of Photo-Optical Instrumentation Engineers (SPIE). [DOI: 10.1117/1.JBO.17.2.025004]

Keywords: biomedical optics; aberrations; vision.

Paper 11436 received Aug. 12, 2011; revised manuscript received Dec. 17, 2011; accepted for publication Dec. 21, 2011; published online Mar. 6, 2012.

## 1 Introduction

There has been interest in peripheral ocular aberrations since the start of the nineteenth century. Most of this has been related to refraction and has been spurred recently by the possibility that the refraction pattern across the visual field may be related to the development of myopia.<sup>1–3</sup> The higher-order aberrations also have received attention in the last dozen years.<sup>4–16</sup>

Investigations of on-axis (foveal) aberrations assume circular pupils, and for most eyes this is a reasonable approximation.<sup>17</sup> A set of circular polynomials, such as Zernike polynomials, is used to describe the wavefronts, and the refractions may be obtained from the coefficients. The assumption of a circular pupil is not reasonable for peripheral vision, however, where the pupil becomes increasingly elliptical with increase in visual field angle. The ratio of the minor to major axes of the ellipse, sometimes called the aspect ratio,  $\epsilon$ , approximates to  $\cos \phi$  over the central field ( $\pm 30$  deg), where  $\phi$  is the off-axis angle (Fig. 1).<sup>18–21</sup> This ellipticity influences the way in which peripheral aberrations are described.

Navarro *et al.*<sup>15</sup> made the first peripheral wavefront estimations, in the nasal visual field, using the laser ray tracing technique. To ensure that the number of positions sampled was the same in both the horizontal and vertical meridians, the horizontal sampling interval was arranged to be  $\cos \phi$  of that in the vertical meridian. The elliptical off-axis pupil was then treated as a circular pupil by normalizing along the major and minor axes of an elliptical pupil. This method, later termed the “stretched ellipse” method by Lundström *et al.*,<sup>7</sup> can also be considered as a “stretching” along the minor axis (Fig. 2). Atchison and

Scott<sup>5</sup> used a Hartmann-Shack wavefront sensor. As they were not able to alter spacing, they had different numbers of sampling positions along the principal meridians. Apart from this, the treatment was similar to that of Navarro *et al.* Provided that the sampling rate is high, this is not a problem. Atchison *et al.*<sup>22–24</sup> described how peripheral refractions could be obtained from the wave aberrations and extended the treatment to consider visual field meridians other than the horizontal meridian.

Lundström *et al.*<sup>7,25</sup> suggested a different approach. Rather than analyzing a stretched elliptical (SE) pupil, they used a circular pupil and analyzed this using Zernike circular polynomials. This pupil can either be enclosed within the elliptical pupil (the small circle or stretched circular (SC) method) or it can have up to the same diameter as the major axis of the elliptical pupil (the large circle or LC method) (Fig. 2). In the latter case, wavefront fits give meaningless data outside the dimensions of the true pupil.<sup>26</sup> Lundström and Unsbo<sup>27</sup> and Lundström *et al.*<sup>7</sup> gave a method for converting the Zernike coefficients obtained with circular pupils (LC method) to those for the SE pupils (SE method) and vice versa. To give a realistic representation of the aberrations with the LC approach, a mask can be placed over wave aberration maps to show only the elliptical region [Figs. 3(a) and 3(b)].

The wavefront aberration reconstruction methods used for the above approaches would usually be based on least-squares fitting of wavefront slopes to spatial derivatives of Zernike polynomials. Wei and Thibos<sup>28</sup> proposed two new methods, inscribed methods and boundary methods, based on the Fourier integral theorem, which they found had accuracy equal to that of least-squares fitting when applied to schematic eyes.

Address all correspondence to: David A. Atchison, Institute of Health and Biomedical Innovation, Queensland University of Technology. Tel: 61 7 31386146; E-mail: d.atchison@qut.edu.au

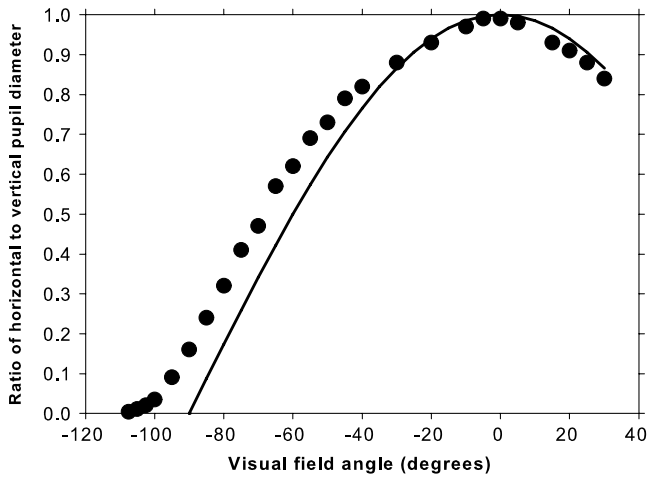


**Fig. 1** Ratio of horizontal to vertical pupil diameters as a function of field angle,  $\phi$ , for dilated pupils (negative angles refer to the temporal field). The continuous curve is a plot of  $\cos \phi$  (after Jay<sup>18</sup>).

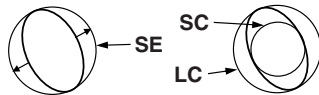


**Fig. 2** Approaches to dealing with pupils in peripheral vision. Left: “stretched” elliptical pupil SE. Right: LC encompassing the elliptical pupil and SC within the elliptical pupil.

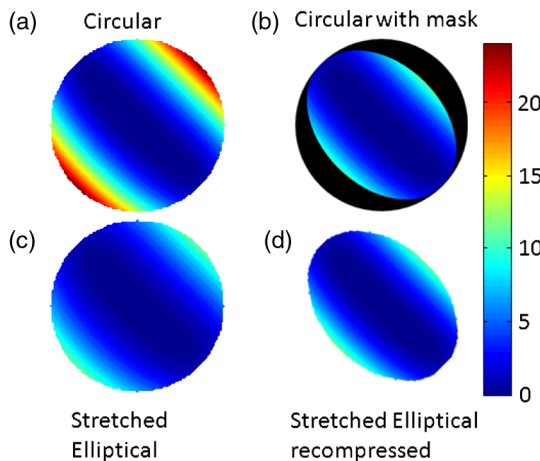


**Fig. 3** Wave aberration maps across the pupil. The left side shows the maps produced by the LC (a) and SE (c) approaches. The LC approach may give meaningless data outside the region of the true pupil; placing a mask with an elliptical aperture over the map gives the correct representation (b). The SE approach gives a distorted map, which may be corrected by recompressing it (d).

There are advantages and disadvantages to both the SE and circular (SC, LC) pupils, as described below (see also Ref. 7). A summary of these points is given in Table 1.

Advantages of the SE pupil approach relative to circular pupil approaches

1. The approach is more physiological than using a circular pupil, as the true off-axis pupil is elliptical or close to elliptical in shape.

2. The aberration polynomials include all the information from the true pupil. This is not the case for a circular pupil with diameter equal to the minor axis of the elliptical pupil (SC method), which fails to make use of all the available data from the natural pupil. The ratio of the area of the SC pupil to that of the full elliptical pupil is equal to the aspect ratio  $\epsilon$  of the ellipse, so that at a field angle of about 40 deg, only about 80% of the available data are used (Fig. 1). When the diameter of the circular pupil exceeds the minor axis of the true pupil (LC method), aberration fitting is meaningless outside the maximum dimensions of the true pupil, as mentioned above. At larger field angles, when the aspect ratio of the elliptical pupil is low, the ratio  $1/\epsilon$  of the area of the LC pupil to that of the true pupil can substantially exceed unity.
3. The root mean square (RMS) wavefront error across the full pupil is given directly by the coefficients  $C_i$  as  $\sqrt{\sum C_i^2}$ . If the same approach is used to calculate the total RMS from the Zernike coefficients for the circular pupils, the result may be too high if the LC approach is used, since spurious contributions will be made by the extrapolated parts of the pupil, and too low if the SC method is employed, since only part of the measured wavefront passing through the natural pupil is used.<sup>7</sup>

4. There is ready compatibility with optical design programs such as Zemax.

Disadvantages of the SE pupil approach relative to circular pupil approaches

1. It is more complicated mathematically, with stretching of the actual and reference imaging positions required, changing the form of auxiliary corrections from spherical to astigmatic wavefront form. Large equations are required to determine refraction equivalents to the wavefront aberrations.<sup>23,24</sup>
2. The shape of the wavefront is distorted by the stretching. When the contours of wavefront error (within an elliptical boundary) are circular, corresponding to defocus or a spherical wavefront, the stretched pupil approach yields astigmatic as well as defocus coefficients.<sup>7,23</sup> As an example, if the refraction correction is a spherical correction +1.01 D for a 5-mm pupil diameter at 40 deg visual field angle along the horizontal field, the SE approach gives defocus coefficient  $C_2^0 = -0.72 \mu\text{m}$  and astigmatism coefficient  $C_2^2 = +0.27 \mu\text{m}$ , whereas the LC approach gives  $C_2^0 = -0.91 \mu\text{m}$  and  $C_2^2 = 0 \mu\text{m}$  (Fig. 4).
3. Should it be decided that the off-axis pupil shape needs correcting (e.g., because the most circular natural pupil is found at a nonzero field angle rather than on the visual axis, as is suggested in Fig. 1), the stretched pupil approach requires calculations to be repeated, whereas the circular pupil approach will require only a different mask.

**Table 1** Advantages and disadvantages of stretched elliptical pupil approach compared with circular pupil approach.

Advantage	Disadvantage	Comment
1. True off-axis pupil is quasi-elliptical-approach is more physiological than using circular pupils.	More complicated mathematically: stretching of real and reference image positions required; spherical power correction has astigmatic coefficients, complicated equations to determine refraction equivalents.	
2. Aberration polynomials include all information from true pupil: SC does not use all data; LC meaningless outside dimensions of true pupil <sup>a</sup>	Shape of wavefront distorted by stretching <sup>b</sup>	<sup>a</sup> Elliptical mask can be used to show wave aberrations and MTF, PSF calculations <sup>b</sup> Wave aberration maps can be rotated and compressed as necessary
3. Root-mean square (RMS) across full elliptical pupil is given directly by coefficients as $\sqrt{(\sum C_i^2)}$ . Estimates too high with LC, too low with SC	Should shape need correcting (e.g., cosine correction not accurate), calculations must be repeated	
4. Compatibility with optical design programs eg., Zemax <sup>a</sup>	Pupil may not longer be elliptical at large angles, and the only reasonable comparison between eyes is provided by aberrations based on circular pupils.	<sup>a</sup> For LC and SC, use elliptical on-axis pupil that looks circular off-axis
5	Comparing coefficients for different angles may not be valid: stretching changes their values differently <sup>b</sup>	<sup>b</sup> It might be considered that this is equally a problem for coefficients with LC and SC approaches
6	Two-dimensional MTFs and PSFs will be distorted if derived directly from wave aberration coefficients <sup>b</sup>	<sup>b</sup> Stretching/compression can compensate. Corrections needed also for LC/SC approaches

<sup>a</sup>in Advantage column refers to a comment in 3rd column.

<sup>b</sup>in Disadvantage column refers to a comment in 3rd column.

4. The underlying assumption of the SE approach, that the natural pupil is elliptical, as given at advantage point 1, may not hold at larger field angles. Jay<sup>18</sup> showed that not only did the ratio of the minor to major pupil diameters fail to follow a  $\cos \phi$  relationship (Fig. 1) but also that the pupil area was slightly greater than would be expected from an ellipse with the same ratio of diameters. A recent computer simulation using a rotationally symmetrical model eye found that, compared with the actual stop (the aperture

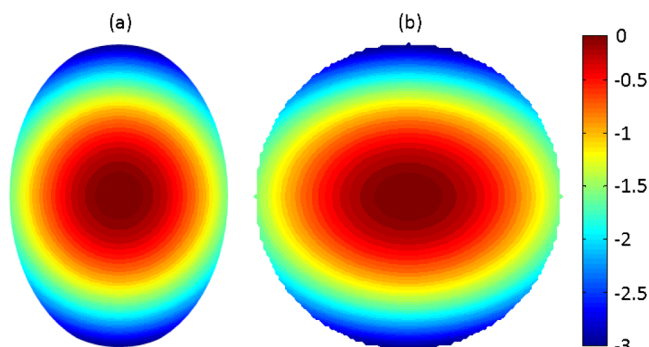


**Fig. 4** Transformation of a rotationally spherical wavefront on an elliptical pupil (a) to a wavefront on a circular pupil according to the SE method (b). The scale bar gives the wavefront aberration in micrometers. The coefficients of the stretched wavefront aberration are defocus  $C_2^0 = -0.72 \mu\text{m}$  and astigmatism  $C_2^2 = +0.27 \mu\text{m}$  (5-mm pupil). Visual field angle is 40 deg.

of the iris), with increasing angle the entrance pupil moves forward, tilts, and does not remain in a plane. This causes the entrance pupil to undergo asymmetric changes in shape, and its geometrical center does not represent precisely the center of the stop.<sup>29</sup>

5. Comparing coefficients for different field angles may not be valid because the stretching of the pupil changes their values differently. This is related to point 2. However, it might equally be considered that there is a problem of validity for the coefficients for circular pupils (SC or LC) because these do not correspond to the natural pupil's shape.
6. Two-dimensional modulation transfer functions and point-spread functions will be distorted if derived directly from the wavefront data for the stretched pupil.

Some of the problems noted above are not as important as they might seem. For example, the issue of the LC circular pupil containing meaningless information (advantage point 2) can easily be negated when showing the wavefront error or calculating image quality criteria such as the modulation transfer function by placing an elliptical mask over the LC circular pupil (Fig. 3, top). The problem of using optical design software for off-axis circular pupils (advantage point 4) can be overcome by using an elliptical on-axis pupil, which appears to be circular when viewed off axis (the ellipticity of the on-axis pupil depends upon the off-axis angle). The second disadvantage is not really a problem when showing wavefront maps, as the wavefront maps can be rotated and compressed as necessary to make them

equivalent to wavefront aberration maps using circular pupils and a mask (Fig. 3, bottom). The distortions of point spread function (PSF) and modulation transfer function (MTF) when derived directly from elliptical pupil coefficients can be corrected by appropriately stretching the PSF by  $1/\cos \phi$  in the direction of the minor axis of the pupil and compressing the spatial frequency scale of the MTF in the same direction by  $\cos \phi$ .

Another approach, so far little used, is to employ elliptical polynomials rather than circular Zernike polynomials.<sup>30–32</sup> The results of using the two types of polynomial were compared by Dai and Mahajan.<sup>31</sup> The circular pupils were given zeros outside the elliptical pupil, which is somewhat different from having missing data. While both sets gave the same wavefront maps, the lower-order coefficients of the circular pupils changed as higher-order terms were added; i.e., they were not orthonormal.

There is clearly a need to better understand the differences in derived coefficients that might arise when different pupil approaches are used. Lundström *et al.*<sup>7</sup> compared estimates of ocular aberration obtained using the SC, LC, and SE methods at the limited set of field angles of 0 deg, 20 deg, and 30 deg along the horizontal meridian of the nasal visual field (temporal retina) in 43 subjects. We now compare estimates of higher-order aberrations when these are based on either the LC or the SE pupil approaches, across the central 42 deg × 32 deg region of the visual field for real eye data and for a larger field for data from model eyes.

## 2 Methods

Using average data previously collected<sup>12</sup> for a group of 10 emmetropes (mean spherical refraction  $0.11\text{D} \pm 0.50\text{D}$ , mean age  $25 \pm 3$  years), we determined aberration coefficients for the LC and SE approaches across a central 42 deg horizontal by 32 deg vertical visual field. Measurements were made with natural pupils under lighting conditions that were such that the minor axis of the elliptical pupil always exceeded 5 mm. For the elliptical pupil coefficients, we used the full SE approach outlined in Atchison *et al.*<sup>23,24</sup> The Shack-Hartmann image array was expanded along the minor axis of the elliptical pupil by a factor  $1/\cos \phi$  and “stretched” data over a central circular area of diameter 5 mm were analyzed (i.e., the elliptical area of unstretched Shack-Hartmann data used had major and minor axes 5 mm and  $5 \cos \phi$  mm, respectively). To produce 5 mm circular pupil data, the unstretched data from the original Shack-Hartmann array of image points were used within the central 5-mm diameter area. In the analysis, the same equations were used as for the SE approach, but with the visual field eccentricity  $\phi$  and meridional angle  $\alpha$  set to zero.

We also did some modeling using the Liou and Brennan<sup>33</sup> model eye, modified in line with a recent study.<sup>12</sup> We removed the asymmetries in the model by making the visual axis coincide with the optical axis. To simulate the usual way in which aberrations are measured, we set the entrance pupil of the eye as the stop and ray-traced out of the eye. Results were based on 5-mm pupils. Aberrations were explored for an emmetropic eye model with the anterior corneal asphericity changed from the value of  $-0.26$ , as used in the original Liou and Brennan model, to  $-0.08$  to match the mean asphericity of our emmetropic subject group. Ray-tracing was done using the optical design program Zemax. A circular stop gives aberrations corresponding to the SE pupil. An LC off-axis pupil was simulated by using elliptical stops whose dimensions along and at right angles to the visual

field meridian were  $5/\cos \phi$  mm and 5 mm, respectively. An SC off-axis pupil was simulated by using elliptical stops whose dimensions along and at right angles to the visual field meridian were 5 mm and  $5 \cos \phi$  mm, respectively.

## 3 Results

Figure 5 shows some individual aberration coefficients for the emmetropic group as a function of visual field position, derived using the LC (left column) and SE (middle column) pupil approaches. Also shown are the differences between the two sets of coefficients (right column). The aberration coefficients change more rapidly across the visual field for the LC approach because they derive from a greater area of the original natural pupil. However, within the range of visual field angles illustrated, the differences are proportionally small. The aberration coefficients for the SC approach, which are not shown, change less rapidly across the field than for the SE approach, but, again, the differences are proportionally small.

Figure 6 shows horizontal coma and spherical aberration coefficients for one subject between  $-50$  deg (temporal) and  $+30$  deg (nasal) of the horizontal visual field. For horizontal coma, the coefficients for the LC, SE, and SC approaches depart considerably from one another beyond  $\pm 20$  deg, but for spherical aberration the departures are relatively smaller.

Figure 7 shows some aberration coefficients for the model eye over a field of 45 deg radius, as derived using the LC, SE, and SC methods. As in the case of Fig. 5 for the emmetropic subject group and for the single subject in Fig. 6, the results are similar for the LC, SE, and SC pupil approaches out to 20 deg eccentricity. Beyond 20 deg, the rates of change of coefficients are very different for the different pupil approaches, particularly for the defocus and spherical aberration where the LC coefficients increase much more rapidly with field angle than the SE and SC coefficients.

## 4 Discussion

### 4.1 How Important are the Differences Between the Two Approaches?

Because the LC pupil is bigger in area than the pupil with the SE approach having the same major axis diameter, the former will produce the greater rate of change of coefficients across the visual field. We have shown that the differences in the estimates of the aberration coefficients are small out to 20 deg for both the real eyes and theoretical eyes (Figs. 5–7). Hence, within this limited central field, the aberration coefficients are little affected by the choice of approach. Beyond 20 deg from fixation, the coefficients may become quite different, with the LC pupil approach showing the greater rates of change. What holds between the LC pupil approach and the SE approach holds also between the SE approach and the SC pupil approach (Figs. 6 and 7), although the selection of a reference pupil size will have some influence on the relationships, and we have not considered this yet.

Note from Fig. 1 that the most circular pupil is not necessarily found on the visual axis and that the  $\cos \phi$  approximation for the aspect ratio of the elliptical pupil is of limited validity. This factor may demand modification of equations used to determine coefficients or to show wave aberration maps, particularly at larger field angles. As noted earlier, at large angles, it may no longer be valid to consider the pupil shape to be elliptical.<sup>18,29</sup>

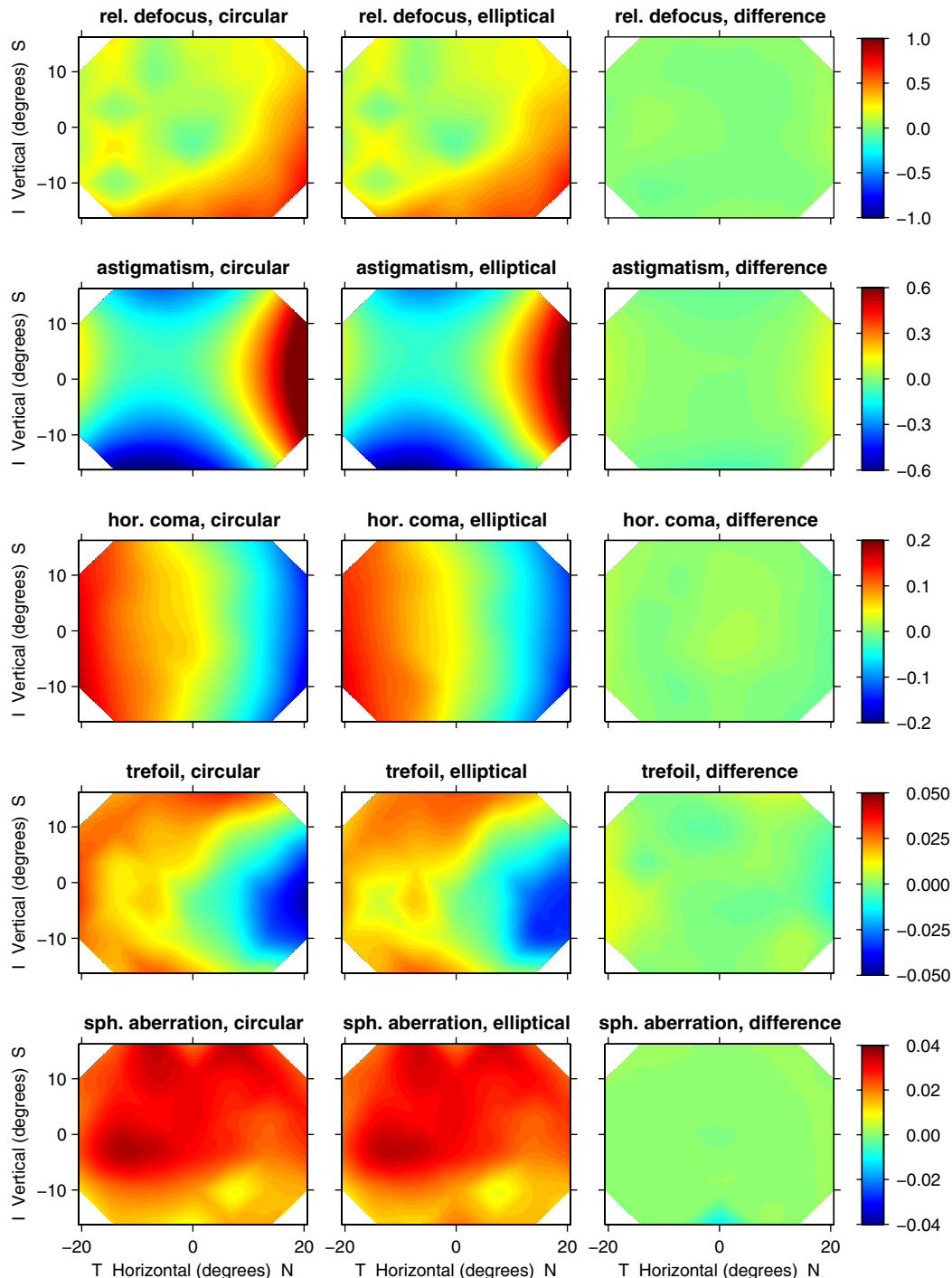


**Fig. 5** Aberration coefficients  $C_2^0$  (for defocus),  $C_2^2$  (astigmatism),  $C_3^1$  (coma),  $C_3^3$  (trefoil) and  $C_4^0$  (spherical aberration) as a function of visual field position for the emmetropic group. Results are shown for (left column) the LC pupil approach and (middle column) the SE pupil approach. The right column shows the differences between the two estimates of the coefficients (i.e., first column—second column). The values for  $C_2^0$  (defocus) are those relative to the on-axis value. Pupil size 5 mm. Note the differences in vertical scales between the different aberrations. *S*: superior field, *I*: inferior field, *T*: temporal field, *N*: nasal field.

#### 4.2 Likely Resolution of this Issue

There is an international standard on aberrations as applied to visual optics<sup>34</sup> that is based on a U.S. standard.<sup>35</sup> This uses Zernike aberrations and circular pupils. In the future, it may be expanded to take into account the noncircular shape of pupils found in peripheral vision. Based on simplicity of use, adequacy of approximation, the fact that pupils viewed off axis may not

always be elliptical, and the desirability of not confusing clinicians, in our opinion the circular approach, using either the LC or SC pupil as appropriate, is preferable to the SE approach for use within the central field of about 30 deg radius. Although it will lead to some loss of information, a variation on the SC pupil is possibly the best choice, with a common pupil size across the range of visual field positions not exceeding the minimum semi-diameter at any of these positions. Our choice of a 30 deg limit is

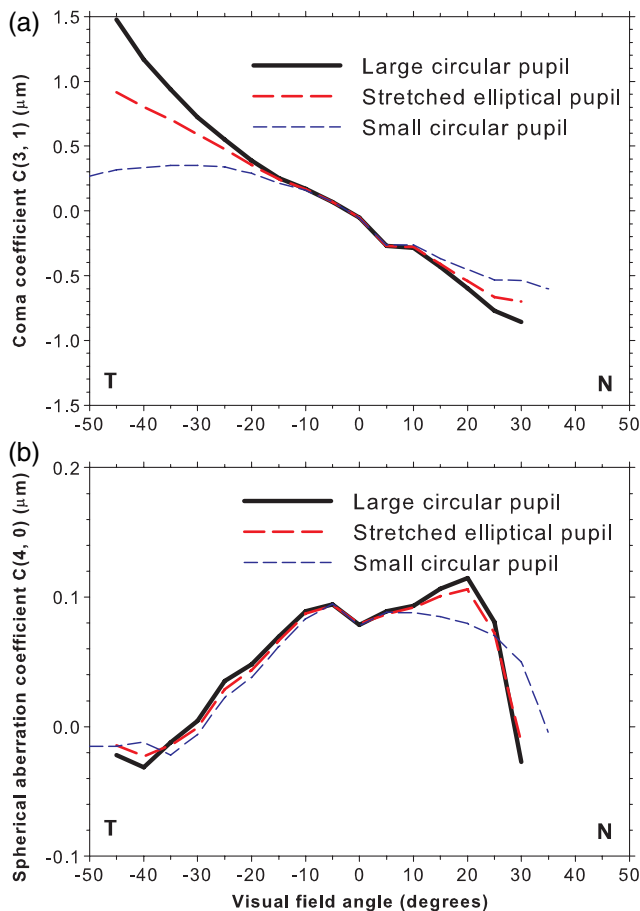


**Fig. 6** Horizontal coma coefficients  $C_{3,1}^0$  (a) and spherical aberration coefficients  $C_{4,0}^0$  (b) for one subject out to 45 deg from fixation along the horizontal meridian. Results are shown for the LC, SE, and SC pupil approaches. Note the differences in vertical scales for the two aberration coefficients. Pupil size is 5 mm. T: temporal field, N: nasal field.

governed by the fact that the relative differences between the areas of the SC and LC pupils and the true elliptical pupil have risen to about 10% to 15%, which seems a reasonable practical tolerance for the approximation. Moreover, 30 deg is about the limit of the field that can be conveniently studied using standard commercial aberrometers.

For studies that extend to field angles in excess of 30 deg, which can easily be achieved with newer laboratory scanning instruments,<sup>36, 37</sup> we suggest that the SE approach be used, with appropriate rescaling of the image plane metrics like the PSF and MTF. We feel that this is necessary because, with increases in field angles beyond 30 deg, the pupil's aspect ratio falls steadily, to reach values of around 0.5 at 60 deg and still smaller values beyond this, so that the circular pupil approximation, whether SC or LC, is no longer adequate. At large field angles, the clinician's familiar circular-pupil-based concepts of mean sphere and astigmatic focal lines with a circle of least confusion dioptrically midway between them are of limited utility.<sup>38</sup>

#### 4.3 Influence of Wavelength on Peripheral Aberrations

Another factor that deserves consideration in relation to the specification of peripheral aberrations is the effect of wavelength.

Aberrations are measured in the near infrared and then corrected for visible wavelengths. For on-axis vision, a correction to the Zernike defocus term  $C_2^0$  based on the Thibos model eye<sup>39</sup> works well:<sup>40</sup>

$$C_{2\lambda}^0 = C_{2\bar{\lambda}}^0 + \frac{633.46R^2(\bar{\lambda} - \lambda)}{4\sqrt{3}(\bar{\lambda} - 214.102)(\lambda - 214.102)}, \quad (1)$$

where the coefficients are in  $\mu\text{m}$ ,  $R$  is the pupil semidiameter (mm),  $\bar{\lambda}$  is the reference wavelength, and  $\lambda$  is the visible wavelength. For other Zernike aberration terms, either the possibility of change in aberrations with wavelength is ignored or corrections are applied that have small effects. As an example of the latter, Abbott Medical Optics applies the following correction for aberration coefficients  $C_n^m$  other than defocus:<sup>23</sup>

$$C_{n\lambda}^m = C_{n\bar{\lambda}}^m \frac{n_\lambda - 1}{n_{\bar{\lambda}} - 1}. \quad (2)$$

Here the refractive index at wavelength  $\lambda$  is that of Thibos' model eye:

$$n_\lambda = 1.320535 + 4.685/(\lambda - 214.102). \quad (3)$$

This equation predicts small relative changes to higher-order aberrations with change in wavelength (2.0% from 842 nm to 550 nm), consistent with the small changes found in experimental results.<sup>40,41</sup>

For off-axis vision, the effect of wavelength on the measured aberrations may differ from that found on axis. In addition, radiation will be incident at an angle to the surface, and this may affect the depth of retinal/choroid penetration for different wavelengths and hence measures of aberration.

There is little information on how the off-axis aberrations are affected by wavelength. Rynders *et al.*<sup>42</sup> used a double-pass method with four subjects to find a trend of longitudinal chromatic aberration between 458 and 633 nm increasing from 1.0 D on axis to 1.5 D at 40 deg horizontal eccentricity. Jaeken *et al.*<sup>43</sup> used the Hartmann-Shack sensor with 11 subjects to find longitudinal chromatic aberration between 473 and 671 nm increasing from 0.97 D on axis to 1.22 D at 30 deg horizontal eccentricity. They also found an increase of astigmatism between 671 nm and 473 nm between fixation and 30 deg of 0.16 D, but there were no significant wavelength-dependent changes in the higher-order aberrations. Transverse chromatic aberration will have a role here because the path of light in the eye is different for different wavelengths for a given object angle. Ogboso and Bedell<sup>44</sup> made measurements of transverse chromatic aberration between 435 and 572 nm along the horizontal visual field. Out to 40 deg object eccentricity, all values were less than 7 min arc for each of four subjects, indicating that transverse chromatic aberration has little effect on the monochromatic aberrations.

On the basis of the limited information currently available, we suggest that at present it is best to treat the effects of wavelength on peripheral aberrations in the same way as those for axial aberrations.

#### 4.4 Visual Field/Retina Reference

Peripheral aberration can be referenced to either the retinal location or to the corresponding visual field position, and there is no clear preference to either in the literature. These are opposite in

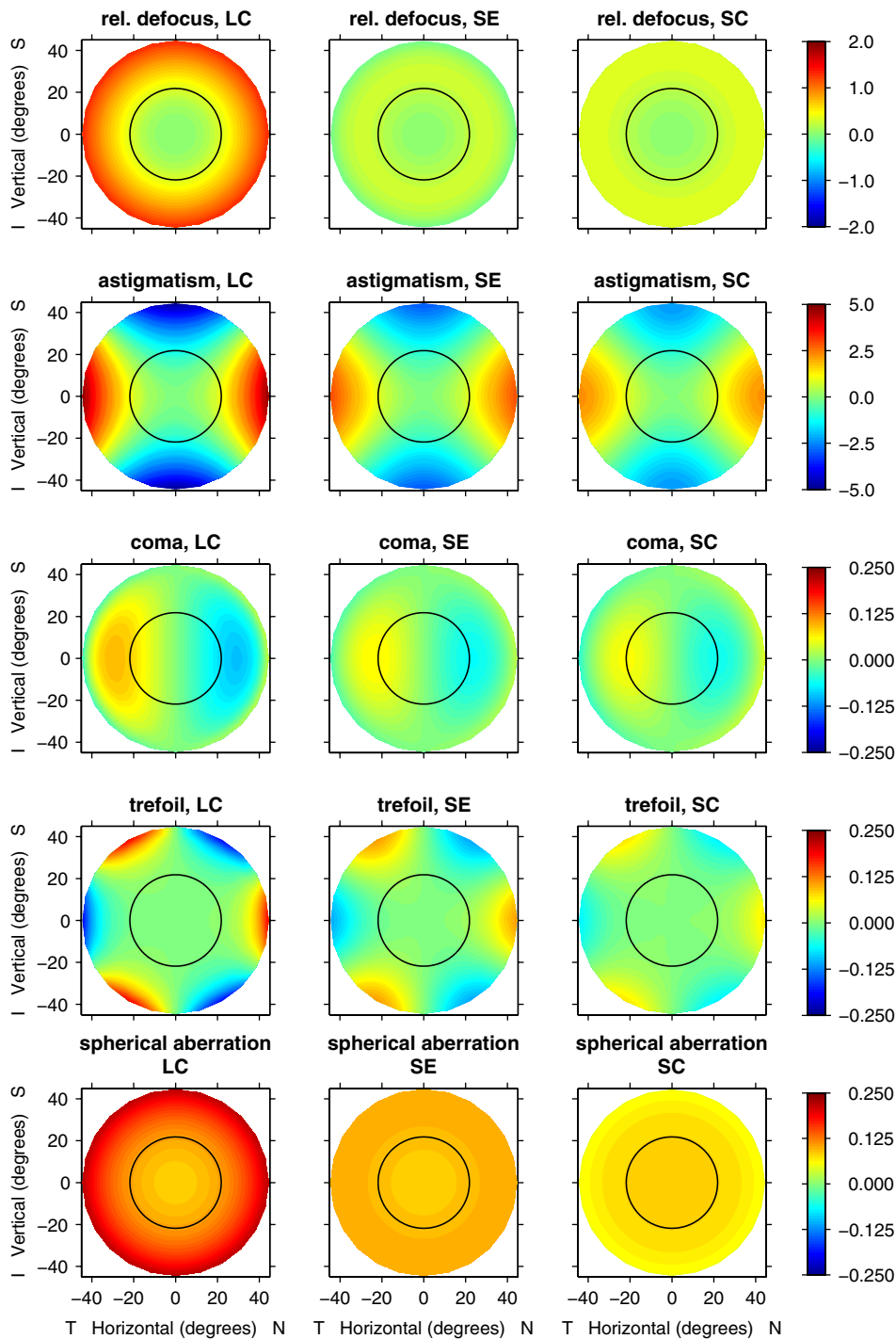


**Fig. 7** Aberration coefficients  $C_2^0$  (for defocus),  $C_2^2$  (for astigmatism),  $C_3^1$  (coma),  $C_3^3$  (trefoil), and  $C_4^0$  (spherical aberration) as a function of visual field position out to 45 deg radius for the emmetropic model eye. Results are shown for (left column) the LC pupil approach, (middle column) the SE pupil approach, and (right column) the SC pupil approach. The values for defocus  $C_2^0$  are those relative to the on-axis value. Pupil size is 5 mm. The black circle encompasses a field radius of 20 deg. Note the differences in vertical scales between the different aberrations. *S*: superior field, *I*: inferior field, *T*: temporal field, *N*: nasal field.

direction to each other; e.g., superior retina corresponds to the inferior visual field. As the actual location on the retina is not known in terms of distance or image side angle relative to the fovea, it might be more appropriate to refer to the visual field position. This can be given in terms of the visual field eccentricity if it is along the horizontal or vertical meridians. For

oblique positions, the visual field eccentricity  $\phi$  and visual field meridian  $\alpha$  can be used, as done here, but it might be appropriate also to refer to the horizontal and vertical components given by

$$\kappa = \tan^{-1}(\tan \phi \cos \alpha), \quad \mu = \tan^{-1}(\tan \phi \sin \alpha). \quad (4)$$

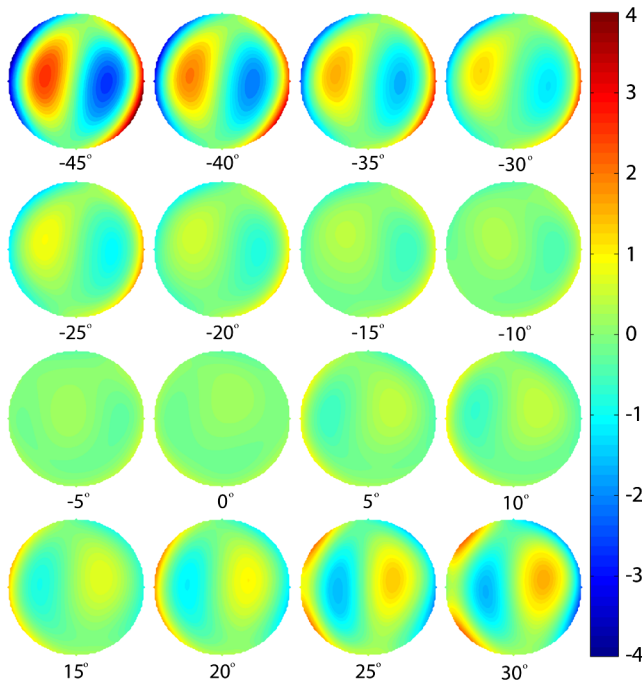


**Fig. 8** Higher-order pupil aberration maps along the horizontal visual field for the subject for whom Fig. 6 shows horizontal coma and spherical aberration coefficients. Results are for 5-mm circular pupils (the LC pupil approach in Fig. 6). The comas are the dominant aberrations. Negative angles correspond to the temporal side of the visual field. The scale gives aberrations in micrometers.

#### 4.5 Sign Convention

In most papers, the nasal visual field/temporal retina and the superior visual field/inferior retina are taken as being positive, and it seems reasonable to continue this. As per positions in the pupil, the ophthalmic optics convention could be adopted so that visual meridian  $\alpha$  is measured anticlockwise from the right side when viewing a subject's eye. The visual field eccentricity does not require a sign.

When comparing aberration coefficients in the visual field between two eyes, or combining data that may be taken from the right eyes of some subjects and the left eyes of others, the expected symmetry of aberrations about the vertical field axis should be taken into account. The correction needed is just that of the positions in the pupil.<sup>34</sup> The signs of left eye coefficients are altered for which the Zernike polynomial functions have negative, even  $m$  indices or positive, odd  $m$  indices.

#### 4.6 Pictorial Representation of Data

Wavefront aberrations can be shown in different ways. To show variation across the field, we have used two approaches. One of these is to generate field maps of individual wave aberration coefficients (Figs. 5–7). Another approach is to plot pupil aberration maps at different individual locations in the visual field.<sup>4, 9–13</sup> Figure 8 shows examples of these along the horizontal field meridian for the subject whose coma and spherical aberration coefficients are shown in Fig. 6.

The two-dimensional field maps (Figs. 5 and 7) have the advantage that they make it easier to appreciate the symmetry characteristics of the variation in individual aberrations across the field, whereas the individual pupil aberration maps give a

more immediate indication of the extent to which a particular aberration may dominate the overall wavefront errors.

## 5 Conclusions

For field angles up to 20 deg, the SE, LC, and SC approaches yield very similar sets of aberration coefficients. At all field angles, the SE and LC pupil approaches give descriptions of off-axis wavefront aberration, which, with appropriate manipulation, lead to the same estimates of PSF, modulation transfer function, or other descriptors of retinal image quality. However, in our opinion, within the field that is currently of main clinical interest (up to about 30 deg radius) the circular pupil approaches are preferable to the SE approach, since they are simpler to implement, they may be more easily understood by clinicians, and pupils viewed off-axis may not always be elliptical. As given above, a variation on the SC pupil is possibly the best choice, with a common pupil size across the range of visual field positions not exceeding the minimum semidiameter at any of these positions. For studies extending to field angles >30 deg, we suggest that the SE approach be used. Since, however, at these large field angles the  $\cos \phi$  approximation for the eccentricity of the approximately elliptical pupils becomes poor, it may be better to use the actual eccentricity in the analysis.

## Acknowledgments

This work was supported by ARC Discovery Grant SP110102018, ARC Linkage Grant LP100100575, and by Carl Zeiss Vision Ltd.

## References

1. J. Hoogerheide, F. Rempt, and W. P. Hoogenboom, "Acquired myopia in young pilots," *Ophthalmologica* **163**(4), 209–215 (1971).
2. R. A. Stone and D. I. Flitcroft, "Ocular shape and myopia," *Ann. Acad. Med. Singapore* **33**(1), 7–15 (2004).
3. J. Wallman and J. Winawer, "Homeostasis of eye growth and the question of myopia," *Neuron* **43**(4), 447–468 (2004).
4. D. A. Atchison et al., "Peripheral ocular aberrations in mild and moderate keratoconus," *Invest. Ophthalmol. Vis. Sci.* **51**(12), 6850–6857 (2010).
5. D. A. Atchison and D. H. Scott, "Monochromatic aberrations of human eyes in the horizontal visual field," *J. Opt. Soc. Am. A* **19**(11), 2180–2184 (2002).
6. A. Guirao and P. Artal, "Off-axis monochromatic aberrations estimated from double pass measurements in the human eye," *Vision Res.* **39**(2), 207–217 (1999).
7. L. Lundström, J. Gustafsson, and P. Unsbo, "Population distribution of wavefront aberrations in the peripheral human eye," *J. Opt. Soc. Am. A* **26**(10), 2192–2198 (2009).
8. L. Lundström, A. Mira-Agudelo, and P. Artal, "Peripheral optical errors and their change with accommodation differ between emmetropic and myopic eyes," *J. Vis.* **9**(6), 17.1–17.11 (2009).
9. A. Mathur and D. A. Atchison, "Effect of orthokeratology on peripheral aberrations of the eye," *Optom. Vis. Sci.* **86**(5), E476–E484 (2009).
10. A. Mathur and D. A. Atchison, "Influence of spherical intraocular lens implantation and conventional laser in situ keratomileusis on peripheral ocular aberrations," *J. Cat. Refract. Surg.* **36**(7), 1127–1134 (2010).
11. A. Mathur, D. A. Atchison, and W. N. Charman, "Effect of accommodation on peripheral ocular aberrations," *J. Vis.* **9**(12), 20.1–20.11 (2009).
12. A. Mathur, D. A. Atchison, and W. N. Charman, "Myopia and peripheral ocular aberrations," *J. Vis.* **9**(10), 15.1–15.12 (2009).
13. A. Mathur, D. A. Atchison, and W. N. Charman, "Effects of age on peripheral ocular aberrations," *Opt. Express* **18**(6), 5840–5853 (2010).

14. A. Mathur, D. A. Atchison, and D. H. Scott, "Ocular aberrations in the peripheral visual field," *Opt. Letters* **33**(8), 863–865 (2008).
15. R. Navarro, E. Moreno, and C. Dorronsoro, "Monochromatic aberrations and point-spread functions of the human eye across the visual field," *J. Opt. Soc. Am. A* **15**(9), 2522–2529 (1998).
16. X. Wei and L. N. Thibos, "Modal estimation of wavefront phase from slopes over elliptical pupils," *Optom. Vis. Sci.* **87**(10), E767–E777 (2010).
17. H. J. Wyatt, "The form of the human pupil," *Vision Res.* **35**(14), 2021–2036 (1995).
18. B. S. Jay, "The effective pupillary area at varying perimetric angles," *Vision Res.* **1**(5–6), 418–424 (1961).
19. K. H. Spring and W. S. Stiles, "Apparent shape and size of the pupil viewed obliquely," *Br. J. Ophthalmol.* **32**(6), 347–354 (1948).
20. K. H. Spring and W. S. Stiles, "Variation of pupil size with change in the angle at which the light stimulus strikes the retina," *Br. J. Ophthalmol.* **32**(6), 340–346 (1948).
21. L. L. Sloan, "The threshold gradients of the rods and the cones; in the dark-adapted and in the partially light-adapted eye," *Am. J. Ophthalmol.* **33**(7), 1077–1089 (1950).
22. D. A. Atchison, D. H. Scott, and W. N. Charman, "Hartmann-Shack technique and refraction across the horizontal visual field," *J. Opt. Soc. Am. A* **20**(6), 965–973 (2003).
23. D. A. Atchison, D. H. Scott, and W. N. Charman, "Measuring ocular aberrations in the peripheral visual field using Hartmann-Shack aberrometry," *J. Opt. Soc. Am. A* **24**(9), 2963–2973 (2007).
24. D. A. Atchison, D. H. Scott, and W. N. Charman, "Measuring ocular aberrations in the peripheral visual field using Hartmann-Shack aberrometry: errata," *J. Opt. Soc. Am. A* **25**(10), 2467 (2008).
25. L. Lundström, P. Unsbo, and J. Gustafsson, "Off-axis wave front measurements for optical correction in eccentric viewing," *J. Biomed. Opt.* **10**(3), 034002.1–034002.7 (2005).
26. J. Shen and L. N. Thibos, "Measuring ocular aberrations and image quality in peripheral vision with a clinical wavefront aberrometer," *Clin. Exp. Optom.* **92**(3), 212–222 (2009).
27. L. Lundström and P. Unsbo, "Transformation of Zernike coefficients: scaled, translated, and rotated wavefronts with circular and elliptical pupils," *J. Opt. Soc. Am. A* **24**(3), 569–577 (2007).
28. X. Wei and L. Thibos, "Design and validation of a scanning Shack Hartmann aberrometer for measurements of the eye over a wide field of view," *Opt. Express* **18**(2), 1134–1143 (2010).
29. C. Fedtke, F. Manns, and A. Ho, "The entrance pupil of the human eye: a three-dimensional model as a function of viewing angle," *Opt. Express* **18**(21), 22364–22376 (2010).
30. G. M. Dai, *Wavefront optics for vision correction*, SPIE Press, Bellingham, Washington USA, pp. 62–69 (2008).
31. G. M. Dai and V. N. Mahajan, "Orthonormal polynomials in wavefront analysis: error analysis," *Appl. Opt.* **47**(19), 3433–3445 (2008).
32. V. N. Mahajan and G. M. Dai, "Orthonormal polynomials in wavefront analysis: analytical solution," *J. Opt. Soc. Am. A* **24**(9), 2994–3016 (2007).
33. H. L. Liou and N. A. Brennan, "Anatomically accurate, finite model eye for optical modeling," *J. Opt. Soc. Am. A* **14**(8), 1684–1695 (1997).
34. International Standards Organisation, "Ophthalmic optics and instruments—Reporting aberrations of the human eye ISO 24157: 2008," (2008).
35. American National Standards Institute, "American National Standard for Ophthalmics—Methods for reporting optical aberrations of the eye," ANSI Z80.28-2004 (2004).
36. J. Taberner and F. Schaeffel, "Fast scanning photoretinoscope for measuring peripheral refraction as a function of accommodation," *J. Opt. Soc. Am. A* **26**(10), 2206–2210 (2009).
37. B. Jaeken, L. Lundstrom, and P. Artal, "Fast scanning peripheral wavefront sensor for the human eye," *Optics Express* **19**(8), 7903–7913 (2011).
38. W. N. Charman and D. A. Atchison, "Optimal spherical focus in the peripheral retina," *Ophthalm. Physiol. Opt.* **28**(3), 269–276 (2008).
39. L. N. Thibos et al., "The chromatic eye: a new reduced-eye model of ocular chromatic aberration in humans," *Appl. Opt.* **31**(19), 3594–3600 (1992).
40. L. Llorente et al., "Aberrations of the human eye in visible and near infrared illumination," *Optom. Vis. Sci.* **80**(1), 26–35 (2003).
41. S. Marcos et al., "A new approach to the study of ocular chromatic aberrations," *Vision Res.* **39**(26), 4309–4323 (1999).
42. M. C. Rynders, R. Navarro, and M. A. Losada, "Objective measurement of the off-axis longitudinal chromatic aberration in the human eye," *Vision Res.* **38**(4), 513–522 (1998).
43. B. Jaeken, L. Lundstrom, and P. Artal, "Peripheral aberrations in the human eye for different wavelengths: off-axis chromatic aberration," *J. Opt. Soc. Am. A* **28**(9), 1871–1879 (2011).
44. Y. U. Ogboso and H. E. Bedell, "Magnitude of lateral chromatic aberration across the retina of the human eye," *J. Opt. Soc. Am. A* **4**(8), 1666–1672 (1987).